Published in final edited form as:
Dev Dyn. 2011 November ; 240(11): 2548–2560. doi:10.1002/dvdy.22741.

Atlas of Wnt and R-Spondin Gene Expression in the Developing Male Mouse Lower Urogenital Tract

Vatsal Mehta[1], **Lisa L. Abler**[1], **Kimberly P. Keil**[1], **Christopher T. Schmitz**[1], **Pinak S. Joshi**[1], and **Chad M. Vezina**[1,*]

[1]University of Wisconsin, Department of Comparative Biosciences

Abstract

Prostate development is influenced by β-catenin signaling, but it is unclear which β-catenin activators are involved, where they are synthesized, and whether their mRNA abundance is influenced by androgens. We identified WNT/β-catenin-responsive β-galactosidase activity in the lower urogenital tract (LUT) of transgenic reporter mice, but β-galactosidase activity differed among the four mouse strains we examined. We used *in situ* hybridization to compare patterns of *Wnts*, r-spondins (*Rspos*, co-activators of β-catenin signaling), β-catenin-responsive mRNAs, and an androgen receptor-responsive mRNA in wild type fetal male, fetal female, and neonatal male LUT. Most *Wnt* and *Rspo* mRNAs were present in LUT during prostate development. Sexually dimorphic expression patterns were observed for WNT/β-catenin-responsive genes, and for *Wnt2b, Wnt4, Wnt7a, Wnt9b, Wnt10b, Wnt11, Wnt16,* and *Rspo3* mRNAs. These results reveal sexual differences in WNT/β-catenin signaling in fetal LUT, supporting the idea that this pathway may be directly or indirectly responsive to androgens during prostate ductal development.

Keywords

Prostate; seminal vesicle; urethra; urogenital sinus; urothelium; vagina; development; mouse; Wnt; R-Spondin

INTRODUCTION

Prostate glandular development begins in male mouse fetuses when prostate ductal progenitors (prostatic buds) are formed in a sub-compartment of the lower urogenital tract (LUT) known as the definitive urogenital sinus (UGS). Prostatic bud formation in C57BL/6J mice occurs between 16–18 days post coitus (dpc) (Lin et al., 2003). Prostatic buds are formed from urothelium, a specialized transitional epithelium in the UGS, and require androgen receptor (AR)-induced signals from UGS stroma (Cunha, 1973; Lasnitzki and Mizuno, 1980; Hayashi et al., 1993). UGSs of male and female fetal mice are capable of forming prostatic buds, provided these tissues are exposed to androgens (Lasnitzki and Mizuno, 1977). Therefore, the female UGS serves as a useful control when identifying androgen-induced genes and signaling pathways contributing to prostate ductal initiation in males.

During perinatal and neonatal development, prostatic buds undergo primary, secondary, and tertiary branching morphogenesis in a pattern unique to each pair of dorsal, ventral, lateral, and anterior rodent prostate lobes (Sugimura et al., 1986). The rate of new ventral prostate

[*]**Correspondence:** Chad M. Vezina, University of Wisconsin-Madison, Dept. Comparative Biosciences, School of Veterinary Medicine, 1656 Linden Drive, Madison, WI 53706, Phone (608) 890-3235, Fax (608) 262-7420, cmvezina@wisc.edu.

ductal tip formation in Balb/c mice, a hallmark of branching morphogenesis, peaks at about postnatal day (P)5 (Sugimura et al., 1986). Concurrent with branching morphogenesis, epithelial buds canalize, giving rise to two distinct cell layers: a superficial layer of secretory columnar luminal epithelium lining prostatic ducts and a deep layer of basal epithelium including the rare neuroendocrine cells (Marker et al., 2003). Basic prostatic architecture is established by puberty and acquires secretory function thereafter (Sugimura et al., 1986). Human prostate development proceeds by a similar series of morphogenetic events, but gives rise to a mature prostate that contains a single capsulated structure divided into peripheral, central, and transitional zones.

The fact that androgens are required for prostatic ductal budding and contribute to branching morphogenesis (Cunha and Lung, 1978) sets the prostate induction mechanism apart from those of most other developing organs. Thus, the developing prostate provides a unique model for investigating how androgens participate in fetal organ development. ARs are located in fetal prostate stroma and epithelium, but only mesenchymal ARs bind testosterone (Shannon and Cunha, 1983) and only in mesenchyme are ARs required for prostatic bud formation (Cunha, 1973; Lasnitzki and Mizuno, 1980; Hayashi et al., 1993). The identity of the androgen-dependent signals produced in fetal prostate mesenchyme and required for prostate ductal development has not yet been determined. However, several signaling pathways have been shown to be active and to collaborate with the AR during prostatic budding and branching morphogenesis. Fibroblast growth factor 10 is essential for prostatic budding and induces epithelial proliferation (Thomson and Cunha, 1999; Kuslak and Marker, 2007). Other factors that positively regulate prostatic budding include epidermal growth factor (Saito and Mizuno, 1997), homeobox genes (Podlasek et al., 1997; Warot et al., 1997), hedgehog signaling (Podlasek et al., 1999; Lamm et al., 2002; Doles et al., 2006; Vezina et al., 2008a), retinoic acid (Vezina et al., 2008a), and SRY box 9 (SOX9) (Thomsen et al., 2008). Negative regulators of prostatic budding include bone morphogenetic proteins 4 and 7 (Grishina et al., 2005; Vezina et al., 2007a) and wingless-related MMTV integration site 5A (WNT5A) (Vezina et al., 2007b). Most of these pathways are not dependent on androgens for their activity in the UGS. It remains to be determined how androgens orchestrate these signaling pathways to pattern prostatic bud formation and later to pattern prostate branching morphogenesis.

β-Catenin, a multi-functional protein that participates in nuclear signaling and cell adhesion, is a candidate for integrating morphogenetic signals during prostate development. β-Catenin is a transcriptional co-activator and downstream component of WNT-mediated signal transduction pathways. It influences the transcriptional activity of many nuclear receptors, including those for androgens, progesterone, vitamin D, retinoic acid, peroxisome proliferators, glucocorticoids, and estrogens (Mulholland et al., 2005). It also assembles complexes containing lymphocyte enhancer factor (LEF), T cell factor (TCF), and other proteins at enhancer sequences on target gene promoters. The gene battery controlled by LEF/TCF is extensive and includes cell cycle regulators, oncogenic transcription factors, tissue remodeling genes, and other factors involved in β-catenin feedback regulation such as *Axin2* and *Lef1* (Filali et al., 2002; Jho et al., 2002; van de Wetering et al., 2002; Willert et al., 2002; Driskell et al., 2004; Klapholz-Brown et al., 2007; Medici et al., 2008). β-Catenin also binds cadherins and, via α-catenin, links their cytoplasmic tails to cytoskeletal actin (Oyama et al., 1994).

β-Catenin has been identified in almost every structure that undergoes a budding program; its activation is necessary and/or sufficient for specification of hair follicle buds (Gat et al., 1998; Lo Celso et al., 2004), mammary gland buds (Faraldo et al., 2006), feather buds (Noramly et al., 1999; Widelitz et al., 2000), and tooth buds (Liu et al., 2008). Whether β-catenin is required for prostatic bud formation has not been determined, but there is evidence

to suggest that at the very least it plays an important role. β-catenin-responsive transcription has been identified in neonatal rat prostate during branching morphogenesis, and ectopic activation of the β-catenin signaling during this period increased prostate cell division and decreased the quantity of ductal branches formed (Wang et al., 2008). Conditional expression of a constitutively active form of β-catenin in developing prostate epithelium has also been shown to prevent epithelial differentiation and promote prostate epithelial hyperplasia (Yu et al., 2009).

Though little knowledge exists about mechanisms controlling β-catenin stabilization during prostate development, WNT genes are likely involved. The WNT superfamily is comprised of at least 19 secreted glycoproteins that serve as short range paracrine signaling effectors. Multiple *Wnt* transcripts have been detected in fetal male UGS by gene expression profiling and many of these transcripts are also present in the adult mouse prostate (Zhang et al., 2006; Schaeffer et al., 2008; Pritchard et al., 2009; Yu et al., 2009; Blum et al., 2010). In fact, functional annotation of mRNAs induced by androgens during mouse prostate development revealed the WNT/β-catenin signaling pathway to be among the most androgen-responsive signaling pathways in the mouse UGS (Schaeffer et al., 2008). Gene expression profiling results have been instrumental for defining which *Wnts* are present in UGS during prostate initiation. This study builds upon previous studies by revealing *Wnt* expression patterns during prostate development.

Members of the R-spondin (*Rspo*) gene family are positive regulators of WNT/β-catenin signaling. They function by binding to the WNT co-receptor low density lipoprotein receptor-related protein 6 and preventing its dikkopf-mediated internalization (Nam et al., 2006). Therefore, RSPOs act in concert with WNTs to stabilize β-catenin. *Rspo* mRNAs are widely distributed during mouse development (Nam et al., 2007). They are required for processes that morphogenetically resemble prostate ductal development, including vascular sprouting (Kazanskaya et al., 2008), limb outgrowth (Aoki et al., 2008), and branching morphogenesis of lung (Bell et al., 2008) and mammary gland (Chadi et al., 2009). *Rspo* expression patterns in the UGS during prostate development have not been assessed previously, to our knowledge, and are a focus of the current study.

The purpose of this study, which was conducted in collaboration with the GenitoUrinary Development Molecular Anatomy Project (GUDMAP, www.gudmap.org), was to characterize patterns of WNT/β-catenin signaling in the male mouse UGS while it undergoes prostatic bud formation and to compare these patterns to the female UGS that does not undergo appreciable prostate development and to the postnatal male prostate while it undergoes branching morphogenesis. Transgenic reporter mice were used to assess WNT/β-catenin-responsive transcriptional activity in the UGS. Wild type mice were used to assess patterns of WNT/β-catenin-responsive mRNAs and the 19 known *Wnt*s and four known *Rspos* that stimulate WNT/β-catenin activity in mouse UGS and neonatal male prostate. Expression patterns were annotated based on a recently described high resolution anatomical ontology for the LUT of mice (Abler et al., 2011a). The ultimate goal was to test the hypothesis that patterns of β-catenin induced gene expression and expression of likely activators of β-catenin exhibit sexual dimorphism indicative of an androgenic mechanism of regulation.

RESULTS

WNT/β-catenin signaling is likely to participate in early stages of prostate ductal development (Wang et al., 2008; Yu et al., 2009; Wu et al., 2011), but it is unclear which cells are involved in this process. Because the LUT is anatomically complex and because it is not known which LUT sub-compartments mediate prostate development, we visualized β-

catenin protein, its downstream transcription targets, and its possible *Wnt* and *Rspo* activators in a spectrum of LUT tissues including bladder neck, pelvic urethra (defined in this study as the urethra spanning the bladder neck and the body wall, including the urogenital sinus [UGS] and, in males, prostatic buds), caudal Wolffian duct (including seminal vesicle and ejaculatory duct) and caudal Müllerian duct (including upper vagina and lower vagina). A schematic diagram illustrating boundaries and selective mRNA markers for each of the male and female mouse LUT anatomical compartments is available in a related publication (Abler et al., 2011a). Our assessments were made at two key prostate development stages: 17 dpc, during initiation of ventral prostatic buds, elongation of anterior prostatic buds, and specification and initiation of dorsolateral prostatic buds (Lin et al., 2003; Vezina et al., 2008b), and P5, near the peak of ventral prostate branching morphogenesis and the initiation of dorsolateral prostate branching morphogenesis (Sugimura et al., 1986).

Immunofluorescent labeling of 17 dpc male and female mouse LUT and P5 male LUT sagittal sections revealed β-catenin protein expression patterns (Fig. 1). Sections were simultaneously immunostained with markers of epithelium, endothelium or smooth muscle, which served as landmarks to localize β-catenin to specific LUT sub-compartments. β-Catenin was detected in cell membranes of urethra urothelium, prostatic bud epithelium, upper and lower vagina epithelium, ejaculatory duct and seminal vesicle epithelium, vascular endothelium, and urethra smooth muscle. We did not detect nuclear β-catenin protein in 17 dpc male or female LUT or in P5 male LUT, even though we were able to detect nuclear β-catenin in a positive control tissue ($Apc^{Min/+}$ mouse colorectal tumor, results not shown) where nuclear β-catenin has been shown previously to exist (Sheng et al., 1998).

Transgenic reporter mice were used to identify LUT cell populations in which β-catenin signaling is likely to be active during prostatic bud formation in 17 dpc males. To determine whether androgens may be involved in WNT/β-catenin signaling, reporter gene activity in 17 dpc males was compared to that of 17 dpc females which do not form large prostatic buds and exhibit less androgen signaling than males (vom Saal, 1989) (Fig. 2). Three random insertion, knock-in reporter mouse lines were used in this experiment: BAT-gal (Maretto et al., 2003), TOPGAL (DasGupta and Fuchs, 1999) and Bat*LacZ* (Nakaya et al., 2005). We also assessed WNT/β-catenin signaling in an *Axin2* reporter mouse line (Lustig et al., 2002) where *LacZ* was targeted to the open reading frame of the β-catenin-responsive *Axin2* (Jho et al., 2002).

WNT/β-catenin-responsive β-galactosidase activity was present in seminal vesicle epithelium and upper vagina epithelium in all four transgenic mouse lines. In two of the mouse lines, β-galactosidase activity was observed in a subset of cells located on the lateral aspects of the pelvic urethra (Fig. 2 A–B, E–F). Pelvic ganglia are located in approximately the same position as the stained cells (Southard-Smith et al., 1998), although it cannot be determined from whole-mount images whether the stained cells are indeed pelvic ganglia. β-galactosidase activity was also detected in the lamina propria region of $Axin2^{Lacz/+}$ males and females (Fig. 2G–H). It was not present in this region of other WNT/β-catenin transgenic reporter mice.

To determine with greater resolution the expression pattern of β-catenin-responsive gene expression, and to assess whether β-catenin or its *Wnt* or *Rspo* activators overlap with androgen receptor (AR)-responsive gene expression, patterns of the WNT/β-catenin-responsive *Axin2* and *Lef1* and the AR-responsive *Srd5a2* were examined in sagittal sections of 17 dpc wild type male and female fetal mouse LUT and P5 male LUT. After ISH staining was completed, sections were co-stained by immunofluorescence with anti-ACTA2

and anti-CDH1 antibodies, which label smooth muscle and epithelium, respectively, to localize mRNAs to specific cell populations. In this and subsequent figures, results for 17 dpc male LUT will be discussed first, possible sexual dimorphism will be revealed by comparing mRNA expression in 17 dpc male and female LUT, and temporal changes in gene expression will be revealed by comparing mRNA expression in 17 dpc male and P5 male LUT. Figure panels are arranged to facilitate mRNA expression pattern comparisons among all three LUTs, with the 17 dpc male serving as the basis for comparison. Descriptions of mRNA expression patterns are based on the anatomical ontology of the Edinburgh Mouse Atlas Project and modifications described by GUDMAP.

Axin2 mRNA expression as assessed in wild type mouse LUT sections by ISH (Fig. 3A–C) generally matched the expression pattern of Axin-dependent β-galactosidase activity in $Axin2^{Lacz/+}$ mouse fetuses (Fig. 2G–H). *Axin2* was abundant in 17 dpc male seminal vesicle epithelium and mesenchyme, lamina propria of the pelvic urethra, basal urothelium of the cranial most aspect of the pelvic urethra, and prostatic bud epithelium and was weakly expressed in muscularis propria (Fig. 3B). While *Axin2* mRNA was abundant in lamina propria of 17 dpc female LUT (Fig. 3A), it was noticeably less abundant in female basal urothelium compared to males. This result reveals a possible sexual dimorphism in WNT/β-catenin signaling in basal urothelial cells that are believed to give rise to prostatic buds in males. *Axin2* mRNA was no longer evident in P5 male pelvic urethra lamina propria, but it persisted in elongating prostatic bud epithelium at this stage (Fig. 3C).

The *Lef1* mRNA expression pattern in 17 dpc LUT overlapped that of *Axin2* mRNA. *Lef1* mRNA was detected in 17 dpc male seminal vesicle epithelium and mesenchyme, lamina propria of the pelvic urethra, basal urothelium of the pelvic urethra, and prostatic bud epithelium and was weakly expressed in muscularis propria (Fig. 3E). Like *Axin2*, *Lef1* was more abundant in male versus female basal urothelium (Fig. 3D–E). Unlike *Axin2*, *Lef1* persisted in lamina propria of P5 male pelvic urethra and was also present during branching morphogenesis in the tips of prostatic buds (Fig. 3F).

Srd5a2 requires androgens and functional androgen receptors for its transcription in mouse UGS (Matsui et al., 2002; Abler et al., 2011a). We previously described the expression pattern of *Srd5a2* in 17 dpc male and female mouse LUT (Abler et al., 2011a). Experiments to localize *Srd5a2* to specific LUT structures were repeated in this manuscript so that *Srd5a2* expression patterns in the male LUT could be compared between two developmental stages (17 dpc and P5) and compared with *Wnt* and *Rspo* mRNA expression patterns. *Srd5a2* mRNA was present in male urethral lamina propria, peri-prostatic mesenchyme, seminal vesicle mesenchyme, and ejaculatory duct mesenchyme (Fig. 3H). *Srd5a2* mRNA was not detected in lamina propria of 17 dpc female pelvic urethra, but it was present in a small compartment of mesenchyme located on the dorsal aspect of the lower vagina (Fig. 3G). *Srd5a2* was present in lamina propria of prostatic urethra, seminal vesicle mesenchyme, ejaculatory duct mesenchyme, and peri-prostatic mesenchyme of the P5 male LUT (Fig. 3I).

We next assessed expression patterns of *Wnt* mRNAs in developing mouse LUT. Weak *Wnt1* mRNA expression was detected in mesenchyme of 17 dpc male and female mouse LUT (Fig. 4A–B) but was not detected in P5 male LUT (Fig. 4C).

Wnt2 mRNA was restricted to lamina propria of the dorsal aspect of 17 dpc male pelvic urethra and was also present in mesenchyme surrounding prostatic buds and seminal vesicle in 17 dpc males (Fig. 4E). Like in 17 dpc males, *Wnt2* mRNA was more prominent in lamina propria of the dorsal versus ventral aspect of 17 dpc female (Fig. 4D) and P5 male pelvic urethra (Fig. 4F). Unlike in 17 dpc males, *Wnt2* was also identified in urothelium of

the caudal aspect of the pelvic urethra and in seminal vesicle epithelium of P5 males (Fig. 4F).

Wnt2b was present in 17 dpc male intermediate and superficial epithelium and was also detected in lamina propria, seminal vesicle mesenchyme, seminal vesicle epithelium, and a portion of the muscularis propria (Fig. 4H). *Wnt2b* was less abundant in 17 dpc male versus female LUT. Sexually dimorphic *Wnt2b* expression was particularly evident in lamina propria of the dorsal aspect of the pelvic urethra (Fig. 4G–H, asterisks). In contrast to 17 dpc males, *Wnt2b* was not detected in P5 male urothelium, but was observed in the submucosal mesenchyme of pelvic urethra and in peri-prostatic mesenchyme surrounding ventral buds (Fig. 4I).

Wnt3 was not detected in 17 dpc male or female LUT, nor was it detected in P5 male LUT (Fig. 4J–L).

Wnt3a mRNA was nearly ubiquitous in 17 dpc male and female LUT (Fig. 5A–B), but was relatively more abundant in distal tips of elongating prostatic buds compared to elsewhere in the P5 male LUT (Fig. 5C).

Wnt4 was localized to intermediate and superficial urothelium of 17 dpc male LUT (Fig. 5E) and exhibited sexually dimorphic expression. It was noticeably less abundant in female compared to male urothelium (Fig. 5D–E, asterisks). The *Wnt4* expression pattern was also different during prostatic bud formation in 17 dpc male compared to during branching morphogenesis in P5 males. *Wnt4* was excluded from prostatic buds in 17 dpc males, but was present in the proximal aspect of prostatic and urethral buds in P5 males (Fig. 5F).

The *Wnt5a* expression pattern was described previously in 17 dpc male mouse LUT, where it was shown to inhibit ventral prostatic bud formation (Allgeier et al., 2008). However, it had not been detailed in 17 dpc female mouse LUT. In 17 dpc males and females, *Wnt5a* mRNA was present in lamina propria and submucosa of the pelvic urethra (Fig. 5G–H). It persisted in these regions during prostatic ductal branching morphogenesis in P5 male LUT (Fig. 5I).

Although *Wnt5a* and *Wnt5b* are paralogs (Katoh, 2005) and sometimes elicit similar responses (van Tienen et al., 2009), their LUT expression patterns were different. In 17 dpc male LUT, *Wnt5b* mRNA was concentrated in submucosal mesenchyme of the pelvic urethra and was relatively more abundant in a restricted zone of mesenchyme located on the dorsal aspect of the bladder neck (Fig. 5K). Weak *Wnt5b* mRNA signal was also localized to seminal vesicle mesenchyme, prostatic bud epithelium, and portions of the ventral mesenchymal pad (VMP, Fig. 5K, dashed lines) which is known to synthesize prostate bud inducing signals including fibroblast growth factor 10 (Thomson and Cunha, 1999). The *Wnt5b* expression pattern in 17 dpc male LUT was similar to the 17 dpc female (Fig. 5J), but different than the P5 male. Most notably, *Wnt5b* mRNA was present in lamina propria and concentrated in mesenchyme of prostatic bud distal tips of the P5 male LUT (Fig. 5L).

Wnt6 mRNA was localized to basal urothelium, prostatic bud epithelium, seminal vesicle epithelium, and superficial urothelium of the caudal aspect of the 17 dpc male pelvic urethra (Fig. 6B). The *Wnt6* mRNA expression pattern was similar in 17 dpc male and female pelvic urethra (Fig. 6A), but differed from P5 males, where it localized to basal urothelium of the urethra and epithelium of the proximal portion of prostatic ducts (Fig. 6C). Also in P5 males, *Wnt6* was present in seminal vesicle epithelium, but in a spotted pattern that differed from the ubiquitous seminal vesicle expression pattern of 17 dpc males.

The *Wnt7a* mRNA expression pattern was described previously in 17 dpc male and female LUT (Abler et al., 2011a), and exhibited a sexually dimorphic pattern (Fig. 6D–E, asterisks). It is important to note that while it was detected in 17 dpc male ductus deferens (Fig. 6E), it was not detected in P5 male LUT (Fig. 6F).

Wnt7b mRNA was present in seminal vesicle epithelium and superficial and intermediate urothelium of 17 dpc male pelvic urethra, but notably was not detected in pelvic urethra basal urothelium. Interestingly, *Wnt7b* was localized to the proximal portion of prostatic ductal epithelium but not detected in the distal tips (Fig. 6H). This result reveals possible *Wnt7b* gene expression differences along elongating prostatic bud axes. *Wnt7b* mRNA expression in the 17dpc male pelvic urethra did not differ from the 17 dpc female (Fig. 6G) or the P5 male (Fig. 6I).

Wnt8a was not detected in 17 dpc male and female LUT (Fig. 6J–K) but was localized to the proximal portion of prostatic duct epithelium in P5 males (Fig. 6L).

Wnt8b, on the other hand, was not detected in any structure of the 17 dpc male, 17 dpc female, or P5 male (Fig. 7A–C).

Wnt9a was localized to lamina propria of 17 dpc male and female LUT (Fig. 7D–E) and was also present in lamina propria of the P5 male LUT (Fig. 7F). In all three tissues, *Wnt9a* was relatively more abundant in the ventral compared to dorsal pelvic urethra. *Wnt9a* was also present in seminal vesicle mesenchyme of the 17 dpc and P5 male.

Wnt9b was described previously in 17 dpc male and female LUT (Abler et al., 2011a) and exhibited sexual dimorphism (Fig. 7G–H, asterisks). It appeared to be restricted to seminal vesicle epithelium of the 17 dpc male and was not detected in the 17 dpc female LUT. Seminal vesicle epithelium expression of *Wnt9b* mRNA appeared to dissipate during neonatal development and exhibited a spotted pattern in the P5 male (Fig. 7I).

Wnt10a mRNA was restricted to basal urothelium of the 17 dpc male pelvic urethra, where it exhibited a spotted expression pattern (Fig. 7K). *Wnt10a* also exhibited a spotted expression pattern in basal urothelium of the 17 dpc female (Fig. 7J) and P5 male pelvic urethra (Fig. 7L).

We recently identified *Wnt10b* as a selective prostatic bud marker in the 17 dpc male LUT (Abler et al., 2011a). *Wnt10b* mRNA was present in ventral, anterior, and dorsolateral prostatic buds at 17 dpc, but since it was restricted to prostatic bud tips, it is not evident in all prostatic buds shown in Fig. 8B. *Wnt10b* was not detected in ejaculatory duct or other epithelial structures within the male LUT. *Wnt10b* expression was less abundant in the 17 dpc female LUT and was restricted to a small region of dorsal urothelium in the pelvic urethra (Fig. 8A), therefore displaying sexual dimorphism (Fig. 8A–B, asterisks). *Wnt10b* remains a selective prostatic bud marker during branching morphogenesis where it was present in distal tips of prostatic buds in the P5 male and was not detected in other structures of the P5 male LUT (Fig. 8C).

Wnt11 mRNA exhibited a diffuse, low-level expression pattern in mesenchyme of the 17 dpc male LUT (Fig. 8E) as well as the 17 dpc female (Fig. 8D). A possible sexually dimorphic expression pattern was observed for *Wnt11* mRNA in the 17 dpc VMP (Fig. 8D–E, dashed lines), where it was more abundant in males compared to females (Fig. 8D–E, asterisks). A small population of *Wnt11*-positive cells was observed in the ventral portion of the P5 male pelvic urethra, distal to the ACTA2-positive muscularis propria (Fig. 8F).

Wnt16 mRNA was restricted to lamina propria and submucosa in the caudal aspect of the 17 dpc (Fig. 8H) and P5 (Fig. 8I) male pelvic urethra. Sexually dimorphic expression of *Wnt16* was evident because it was not detected in lamina propria and submucosa of the 17 dpc female pelvic urethra and was instead present in female urethra urothelium (Fig. 8G, asterisk).

All four known *Rspo* mRNAs were present at the time of prostatic bud formation in the 17 dpc male LUT (Fig. 9), although each of their expression patterns was unique. *Rspo1* mRNA was detected in the VMP, the anterior mesenchymal pad, and portions of lamina propria and seminal vesicle mesenchyme of the 17 dpc male LUT (Fig. 9B). The *Rspo1* expression pattern was similar in 17 dpc male and female LUT (Fig. 9A–B. However, although *Rspo1* was not detected in 17 dpc prostatic buds, it was present at P5 in distal prostatic bud tips (Fig. 9C).

Rspo2 mRNA was predominantly located in mesenchymal pads of the 17 dpc male and female pelvic urethra (Fig. 9 D–E, dashed lines) and was not detected in the P5 male LUT (Fig. 9F).

Rspo3 was present in mesenchymal pads of the pelvic urethra and in seminal vesicle mesenchyme of the 17 dpc male (Fig. 9H). Interestingly, *Rspo3* showed a sexually dimorphic pattern of expression at 17 dpc: it was detected in male VMP (Fig. 9H, dashed lines) but not in female VMP (Fig. 9G, dashed lines). The presence of *Rspo3* mRNA in mesenchymal pads and seminal vesicle mesenchyme persisted from 17 dpc until at least P5 (Fig. 9I).

Rspo4 mRNA was detected in mesenchyme of 17 dpc male and female LUT (Fig. 9 J–K) and although it was not detected in prostatic buds at 17 dpc, it was present in the distal tips of prostatic buds at P5 (Fig. 9L).

DISCUSSION

We provide three pieces of evidence supporting the hypothesis that β-catenin participates in mouse prostatic bud formation. First, we identified β-catenin protein as being present in prostatic bud epithelium and other fetal urothelium that gives rise to prostatic buds. Second, WNT/β-catenin-responsive transcriptional target genes *Axin2* and *Lef1* are prominent in prostatic bud epithelium and are noticeably more abundant in basal urothelium of males compared to females. Third, many potential activators of β-catenin are present in the male and female UGS. Five of these potential β-catenin activators (*Wnt4*, *Wnt10b*, *Wnt11* *Wnt16*, and *Rspo3*) appear to be more abundant in male versus female UGS, indicating they may be responsive to androgenic regulation. Together, these results highlight a need for additional studies to address if and how ARs interface with WNTs, RSPOs, and β-catenin signaling to stimulate prostatic development.

While most of our data support a role for β-catenin serving as a transcriptional co-activator in prostatic buds, there were some discrepant results. These results are useful to the prostate development research community because they reveal methodological approaches that are not likely to be informative for studying β-catenin signaling in the fetal mouse LUT. One of the discrepant results involves nuclear localization of β-catenin. Nuclear β-catenin is required for WNT/β-catenin signaling, but nuclear β-catenin protein was not detected in immunofluorescently stained fetal mouse LUT sections. Others have also reported difficulty in detecting nuclear β-catenin in developing tissues where it is required for WNT/β-catenin signaling (Anderson et al., 2002; Murtaugh et al., 2005). In line with these studies, we were unable to detect nuclear β-catenin in developing seminal vesicles between 13 dpc-birth (results not shown), even though β-catenin has been confirmed previously to be an essential

mediator of WNT signaling in seminal vesicles during this embryonic period (Marose et al., 2008). The fact that endogenous WNT signaling translocates only a fraction of the total cellular β-catenin to the nucleus, and that the conformation of nuclear beta-catenin protein may render it a poor antigen for the antibody used in this study are both plausible reasons for our inability to detect it in developing mouse LUT nuclei. As Consequently, nuclear localization of β-catenin is not likely to be a sensitive readout for β-catenin signaling in the developing mouse prostate, at least not in the C57BL/6J mouse strain and at the developmental stages (17 dpc, P5) that were investigated here.

We were unable to visualize WNT/β-catenin reporter activity in urethra lamina propria and prostatic bud epithelium in three random insertion, knock-in reporter mouse lines that have been used in other developing tissues to localize WNT/β-catenin signaling: Bat*LacZ* (Nakaya et al., 2005), BAT-gal (Maretto et al., 2003) and TOPGAL (DasGupta and Fuchs, 1999). The targeting vectors used to generate all three strains were similar in that they contained the full-length *LacZ* gene and a minimal promoter driven by multimeric TCF/LEF enhancer sequences. The mouse strains differ in the number of TCF/LEF enhancer sites contained in each targeting vector and in the genomic integration sites of the targeting vectors. While *LacZ* staining activity was observed in the LUT of all three mouse lines, especially in Müllerian and Wolffian duct-derived epithelium, none showed high fidelity *LacZ* activity in urethral lamina propria mesenchyme or UGS urothelium. Reporter mouse strains are not infallible; there are well recognized discrepancies in WNT/β-catenin reporter gene expression patterns among these transgenic mouse lines, and it is also known that the mouse lines sometimes fail to detect WNT/β-catenin activity in tissues where it has been shown to exist (Barolo, 2006). While Bat*LacZ*, BAT-gal and TOPGAL mouse models are excellent reporters of β-catenin signaling in other tissues, they do not appear to be sensitive reporters of β-catenin signaling in 17 dpc and P5 C57BL/6J developing mouse prostate.

We also assessed WNT/β-catenin signaling in an *Axin2* reporter mouse line where *LacZ* was targeted to the *Axin2* reading frame (Lustig et al., 2002). We observed abundant *Axin2*-dependent *LacZ* activity in lamina propria of 17 dpc male and female LUT and in prostatic bud epithelium of males. These results are corroborated by mRNA expression pattern of the endogenous *Axin2* gene, and the mRNA expression pattern of *Lef1*, also a WNT/β-catenin-responsive gene. The fact that the *Axin2* reporter mouse strain was created by a targeted insertion, versus the random insertion method of the other WNT/β-catenin reporter strains, could be an important reason why *LacZ* staining was detected in *Axin2* reporter mouse UGS and not in other strains.

β-catenin protein is not abundant in lamina propria. In fact, we were unable to detect it in this tissue compartment by immunofluorescence. Although it remains possible that low levels of β-catenin protein coactivate WNT/β-catenin signaling in lamina propria, it is also possible that lamina propria *Axin2* and *Lef1* are regulated by a non-WNT/β-catenin mechanism.

One of the most interesting results in this study was the identification of sexually dimorphic transcription of WNT/β-catenin-responsive genes in UGS epithelium. Both *Axin2* and *Lef1* mRNA were abundant in prostatic bud epithelium at 17 dpc, a region where β-catenin protein is also abundant, supporting the idea that WNT/β-catenin signaling is selectively activated in developing prostatic buds and in nearby basal urothelium. These results are strong evidence of a link between androgen activity in fetal UGS stroma and WNT/β-catenin signaling in fetal prostatic buds. Whether β-catenin is required for prostatic bud formation and whether androgens are required for WNT/β-catenin signaling remains to be determined.

There are several possibilities for why WNT/β-catenin signaling is selectively activated in male prostatic bud epithelium. One possibility is that male UGS contains fewer WNT beta-catenin signaling compared to female UGS. The beta-catenin signaling inhibitors dickkopf homolog (DKK) 1 and 3 have been shown to impair adult prostate epithelial cell proliferation (Kawano et al., 2006; Hall et al., 2010), although it is unclear whether DKKs exert the same action on fetal prostate or whether they are negatively regulated by androgens in the fetal prostate. Exogenous DKK1 has also been shown to decrease the number of prostatic tips formed in mouse UGS organ culture, suggesting an inhibition of prostate branching morphogenesis (Wang et al., 2008). Secreted frizzled related protein 1 (SFRP1), also an inhibitor of WNT/- β-catenin signaling, has been shown to impair prostatic bud formation and branching morphogenesis (Joesting et al., 2008) but it is not known whether SFRP1 is regulated by androgens.

Wnt and *Rspo* activators of β-catenin could also be responsible for activating β-catenin-dependent transcription in prostatic buds, and these molecules were the focus of the current study. We identified a surprising quantity of these mRNAs in developing mouse LUT. 15 *Wnt* and 4 *Rspo* mRNAs were present in the 17 dpc female LUT, 16 *Wnt* and 4 *Rspo* mRNAs were detected in male LUT at the same fetal stage, and 15 *Wnt* and 3 *Rspo* mRNAs were observed in the P5 male LUT.

ISH results in the current study, like all ISH studies, are subject to several limitations. Off-target riboprobe binding could have caused some *Wnts* and *Rspos* to be falsely identified as present in the UGS and neonatal prostate. ISH is also known to be less sensitive than other methods of mRNA detection, such as RT-PCR, which could have caused some *Wnts* and *Rspos* to be falsely identified as absent in the LUT. Finally, ISH is not a quantitative approach for assessing mRNA expression. Biological and bioinformatic measures were taken to ensure riboprobe specificity and sensitivity and to limit experimental variability among samples. These measures included: selection of unique cDNA sequences for riboprobe synthesis, biological and experimental sample replication for ISH stained sections, and assessment of specific and sensitive mRNA expression in non-LUT positive control tissues that have been shown in other studies to express each *Wnt* or *Rspo* isoform. Confidence in this study's results are strengthened by the fact that they align closely with those of others who used non-ISH methods to assess *Wnt* expression during prostate development. Yu *et al.* (2009) used RT-PCR to identify the presence of 16 *Wnt* mRNAs in the 16 dpc male mouse UGS. Zhang *et al.* (2006) used serial analysis of gene expression to identify 9 *Wnt* mRNAs in the 16 dpc male mouse UGS. Our ISH results for *Wnt* expression overlap those previously reported by Yu *et al.* (2009) and Zhang *et al.* (2006). In all three studies, *Wnt2a, Wnt6*, *Wnt7b*, *Wnt4*, *Wnt7a*, and *Wnt10a* were reported as being present and *Wnt3* and *Wnt8a* were reported as being absent in the male UGS.

Of considerable interest is the fact that multiple possible β-catenin activators were observed in sexually dimorphic expression patterns in mouse LUT during prostatic bud initiation and elongation, including *Wnt2b*, *Wnt4, Wnt7a, Wnt9b* and *Wnt10b, Wnt11, Wnt16, and Rspo3*. Because assessments of these mRNAs were completed at an embryonic stage (17 dpc) when some prostatic buds had already formed, it is not possible to determine whether sexually dimorphic mRNA expression patterns were induced directly by ARs in male UGS mesenchyme, or indirectly by paracrine signaling between prostatic bud epithelium and UGS mesenchyme. Most of the WNTs that were reported to have sexually dimorphic patterns in this study are unlikely to be direct targets of AR signaling. Only mesenchymal ARs are capable of binding to androgens (Shannon and Cunha, 1983) and only in mesenchyme are they required for prostatic bud formation (Cunha, 1973; Lasnitzki and Mizuno, 1980; Hayashi et al., 1993). Since *Axin2*, *Wnt4, Wnt7a, Wnt9b* and *Wnt10b* were detected in urothelium and not UGS mesenchyme, they are unlikely to be direct

transcriptional targets of the mesenchymal AR during prostate development. This does not preclude the possibility that they are indirectly controlled by mesenchymal AR signaling, potentially by the same mesenchymal androgen-dependent signals that stimulate prostatic bud and branching morphogenesis. On the other hand, *Srd5a2*, *Wnt2b, Wnt11, Wnt16,* and *Rspo3* exhibited sexually dimorphic patterns in UGS mesenchyme. *Srd5a2*, *Wnt16,* and *Rspo3* were noticeably more abundant in male versus female UGS mesenchyme, while *Wnt2b* was more abundant in females compared to males. *Srd5a2* is established as an AR target gene in UGS mesenchyme (Abler et al., 2011a), but transcription of the other genes in the UGS has not been identified previously as being responsive to or dependent on AR signaling. The fact that at least one of these mRNAs (*Wnt16*) is positively regulated by androgens in adult human prostate fibroblasts (Tanner et al., 2011) is intriguing and leads to the hypothesis that stromal AR regulation of some *Wnts* and *Rspos* may be conserved throughout prostate development and across species. Additional studies are needed to test these hypotheses and to determine whether activated ARs are necessary and/or sufficient for expression of *Wnt11, Wnt16,* and *Rspo3* in the developing and adult mouse prostate.

EXPERIMENTAL PROCEDURES

Animals

C57BL/6J mice (Jackson Laboratory, Bar Harbor, ME) were housed in clear plastic cages containing corn cob bedding and maintained on a 12 hr light and dark cycle at 25±5°C and 20–50% relative humidity. Feed (Diet 2019 for males and Diet 7002 for pregnant females, Harlan Teklad, Madison, WI) and water were available *ad libitum*. All procedures were approved by the University of Wisconsin Animal Care and Use Committee and conducted in accordance with the NIH Guide for the Care and Use of Laboratory Animals. To obtain timed-pregnant dams, female mice were paired overnight with males. The next day was considered 0 dpc. Dams were euthanized by CO_2 asphyxiation and fetuses were maintained in Hank's Balanced Salt Solution prior to dissection.

Assay for β-galactosidase activity

β-Galactosidase activity was determined as described previously (Cheng et al., 1993). LUTs were fixed for 20 min in ice-cold 4% paraformaldehyde (PFA), rinsed with phosphate buffered saline (PBS), and suspended in PBS containing 5 mM $K_3Fe(CN)_3$, 5 mM $K_4Fe(CN)_6$, 2 mM $MgCl_2$, 0.02% NP-40, 0.01% sodium deoxycholate, and 1 mg/ml X-gal. All tissues were incubated for 18 h at 37 °C in the dark on a rocking platform, washed with PBS, and imaged.

In Situ Hybridization (ISH)

Detailed protocols are available at www.gudmap.org and were described previously (Abler et al., 2011b). Fetal male and female mouse lower urogenital tract (LUT) tissues were fixed overnight at 4°C in PBS containing 4% PFA. Tissues were dehydrated into 100% methanol for archival storage at −20°C and rehydrated prior to sectioning. Tissue sectioning and ISH were conducted as described previously (Abler et al., 2011b). BM Purple was used as an alkaline phosphatase chromagen for detection of digoxigenin-labeled riboprobes. Immunofluorescent staining of ISH-stained sections was conducted as described previously (Abler et al., 2011a). The staining pattern for each hybridized riboprobe was assessed in at least two LUT sections / mouse fetus and at least three litter-independent fetuses. Replicate male and female tissue sections were processed as a single experimental unit to allow for qualitative comparisons among biological replicates and between males and females. Information about the PCR-generated riboprobes used in this study is available in Supplemental Table 1. Detailed annotation of mRNA expression patterns, as well as additional images of ISH-stained tissue sections, are available at www.gudmap.org.

Immunohistochemistry

C57BL/6J mouse tissues were fixed in 4% paraformaldehyde, dehydrated into methanol, infiltrated with paraffin, and cut into 5 μm sections. $Apc^{Min/+}$ mouse intestinal tumors, a positive control for β-catenin IHC, were from Dr. Richard Halberg, University of Wisconsin-Madison, and were described previously (Halberg et al., 2009). After deparaffinization, hydration and antigen unmasking in boiling 10 mM sodium citrate (pH 6), tissues were stained as described (Abler et al., 2011a). Primary antibodies were diluted as follows: 1:250 rabbit anti-CDH1 (#3195, Cell Signaling Technologies, Beverly, MA) and 1:100 mouse anti-CTNNB1 (#610153, BD Transduction Laboratories, Franklin Lakes, NJ). Secondary antibodies were diluted as follows: 1:250 diluted Dylight 488-cojugated anti-mouse IgG (#115-487-003, Jackson Immunoresearch, West Grove, PA) and Dylight 546-counjugated goat anti-rabbit IgG (#111-507-003, Jackson Immunoresearch). Immunofluorecently labeled tissues were counterstained with 4',6-diamidino-2-phenylindole, dilactate and mounted in anti-fade media (phosphate-buffered saline containing 80% glycerol and 0.2% n-propyl gallate).

Supplementary Material

Refer to Web version on PubMed Central for supplementary material.

Acknowledgments

The authors wish to thank Dr. Caroline Alexander and Ms. Catherine Smith, University of Wisconsin-Madison, for providing $Axin2^{LacZ}$ mouse tissues for this study, and Dr. Richard Halberg, University of Wisconsin-Madison, for providing $Apc^{Min/+}$ mouse tumor tissue.

Grant Information: This work was supported by National Institutes of Health Grants DK083425 and DK070219.

REFERENCES

Abler LL, Keil KP, Mehta V, Joshi PS, Schmitz CT, Vezina CM. A High Resolution Molecular Atlas of the Fetal Mouse Lower Urogenital Tract. Dev Dyn. 2011a In Press.

Abler LL, Mehta V, Keil KP, Joshi PS, Flucus C-L, Hardin HA, Schmitz CT, Vezina CM. A high throughput in situ hybridization method to characterize mRNA expression patterns in the fetal mouse lower urogenital tract. J Vis Exp. 2011b In Press.

Allgeier SH, Lin TM, Vezina CM, Moore RW, Fritz WA, Chiu SY, Zhang C, Peterson RE. WNT5A selectively inhibits mouse ventral prostate development. Dev Biol. 2008; 324:10–17. [PubMed: 18804104]

Anderson CB, Neufeld KL, White RL. Subcellular distribution of Wnt pathway proteins in normal and neoplastic colon. Proc Natl Acad Sci U S A. 2002; 99:8683–8688. [PubMed: 12072559]

Aoki M, Kiyonari H, Nakamura H, Okamoto H. R-spondin2 expression in the apical ectodermal ridge is essential for outgrowth and patterning in mouse limb development. Dev Growth Differ. 2008; 50:85–95. [PubMed: 18067586]

Barolo S. Transgenic Wnt/TCF pathway reporters: all you need is Lef? Oncogene. 2006; 25:7505–7511. [PubMed: 17143294]

Bell SM, Schreiner CM, Wert SE, Mucenski ML, Scott WJ, Whitsett JA. R-spondin 2 is required for normal laryngeal-tracheal, lung and limb morphogenesis. Development. 2008; 135:1049–1058. [PubMed: 18256198]

Blum R, Gupta R, Burger PE, Ontiveros CS, Salm SN, Xiong X, Kamb A, Wesche H, Marshall L, Cutler G, Wang X, Zavadil J, Moscatelli D, Wilson EL. Molecular signatures of the primitive prostate stem cell niche reveal novel mesenchymal-epithelial signaling pathways. PLoS One 5Wang X, Zavadil J, Moscatelli D, Wilson EL. 2010. Molecular signatures of the primitive prostate stem cell niche reveal novel mesenchymal-epithelial signaling pathways. PLoS One. 2010; 5

Chadi S, Buscara L, Pechoux C, Costa J, Laubier J, Chaboissier MC, Pailhoux E, Vilotte JL, Chanat E, Le Provost F. R-spondin1 is required for normal epithelial morphogenesis during mammary gland development. Biochem Biophys Res Commun. 2009; 390:1040–1043. [PubMed: 19857464]

Cheng TC, Wallace MC, Merlie JP, Olson EN. Separable regulatory elements governing myogenin transcription in mouse embryogenesis. Science. 1993; 261:215–218. [PubMed: 8392225]

Cunha GR. The role of androgens in the epithelio-mesenchymal interactions involved in prostatic morphogenesis in embryonic mice. Anat Rec. 1973; 175:87–96. [PubMed: 4734188]

Cunha GR, Lung B. The possible influence of temporal factors in androgenic responsiveness of urogenital tissue recombinants from wild-type and androgen-insensitive (*Tfm*) mice. J Exp Zool. 1978; 205:181–193. [PubMed: 681909]

DasGupta R, Fuchs E. Multiple roles for activated LEF/TCF transcription complexes during hair follicle development and differentiation. Development. 1999; 126:4557–4568. [PubMed: 10498690]

Doles J, Cook C, Shi X, Valosky J, Lipinski R, Bushman W. Functional compensation in hedgehog signaling during mouse prostate development. Dev Biol. 2006; 295:13–25. [PubMed: 16707121]

Driskell RR, Liu X, Luo M, Filali M, Zhou W, Abbott D, Cheng N, Moothart C, Sigmund CD, Engelhardt JF. Wnt-responsive element controls Lef-1 promoter expression during submucosal gland morphogenesis. Am J Physiol Lung Cell Mol Physiol. 2004; 287:L752–L763. [PubMed: 15194563]

Faraldo MM, Taddei-De La Hosseraye I, Teuliere J, Deugnier MA, Moumen M, Thiery JP, Glukhova MA. Mammary gland development: Role of basal myoepithelial cells. J Soc Biol. 2006; 200:193–198. [PubMed: 17151555]

Filali M, Cheng N, Abbott D, Leontiev V, Engelhardt JF. Wnt-3A/beta-catenin signaling induces transcription from the LEF-1 promoter. J Biol Chem. 2002; 277:33398–33410. [PubMed: 12052822]

Gat U, DasGupta R, Degenstein L, Fuchs E. De Novo hair follicle morphogenesis and hair tumors in mice expressing a truncated beta-catenin in skin. Cell. 1998; 95:605–614. [PubMed: 9845363]

Grishina IB, Kim SY, Ferrara C, Makarenkova HP, Walden PD. BMP7 inhibits branching morphogenesis in the prostate gland and interferes with Notch signaling. Dev Biol. 2005; 288:334–347. [PubMed: 16324690]

Halberg RB, Waggoner J, Rasmussen K, White A, Clipson L, Prunuske AJ, Bacher JW, Sullivan R, Washington MK, Pitot HC, Petrini JH, Albertson DG, Dove WF. Long-lived Min mice develop advanced intestinal cancers through a genetically conservative pathway. Cancer Res. 2009; 69:5768–5775. [PubMed: 19584276]

Hall CL, Zhang H, Baile S, Ljungman M, Kuhstoss S, Keller ET. p21CIP-1/WAF-1 induction is required to inhibit prostate cancer growth elicited by deficient expression of the Wnt inhibitor Dickkopf-1. Cancer Res. 2010; 70:9916–9926. [PubMed: 21098705]

Hayashi N, Cunha GR, Parker M. Permissive and instructive induction of adult rodent prostatic epithelium by heterotypic urogenital sinus mesenchyme. Epithelial Cell Biol. 1993; 2:66–78. [PubMed: 8353595]

Jho EH, Zhang T, Domon C, Joo CK, Freund JN, Costantini F. Wnt/beta-catenin/Tcf signaling induces the transcription of Axin2, a negative regulator of the signaling pathway. Mol Cell Biol. 2002; 22:1172–1183. [PubMed: 11809808]

Joesting MS, Cheever TR, Volzing KG, Yamaguchi TP, Wolf V, Naf D, Rubin JS, Marker PC. Secreted frizzled related protein 1 is a paracrine modulator of epithelial branching morphogenesis, proliferation, and secretory gene expression in the prostate. Dev Biol. 2008; 317:161–173. [PubMed: 18371946]

Katoh M. Comparative genomics on Wnt5a and Wnt5b genes. Int J Mol Med. 2005; 15:749–753. [PubMed: 15754042]

Kawano Y, Kitaoka M, Hamada Y, Walker MM, Waxman J, Kypta RM. Regulation of prostate cell growth and morphogenesis by Dickkopf-3. Oncogene. 2006; 25:6528–6537. [PubMed: 16751809]

Kazanskaya O, Ohkawara B, Heroult M, Wu W, Maltry N, Augustin HG, Niehrs C. The Wnt signaling regulator R-spondin 3 promotes angioblast and vascular development. Development. 2008; 135:3655–3664. [PubMed: 18842812]

Klapholz-Brown Z, Walmsley GG, Nusse YM, Nusse R, Brown PO. Transcriptional program induced by wnt protein in human fibroblasts suggests mechanisms for cell cooperativity in defining tissue microenvironments. PLoS ONE. 2007; 2:e945. [PubMed: 17895986]

Kuslak SL, Marker PC. Fibroblast growth factor receptor signaling through MEK-ERK is required for prostate bud induction. Differentiation. 2007; 75:638–651. [PubMed: 17309601]

Lamm ML, Catbagan WS, Laciak RJ, Barnett DH, Hebner CM, Gaffield W, Walterhouse D, Iannaccone P, Bushman W. Sonic hedgehog activates mesenchymal Gli1 expression during prostate ductal bud formation. Dev Biol. 2002; 249:349–366. [PubMed: 12221011]

Lasnitzki I, Mizuno T. Induction of the rat prostate gland by androgens in organ culture. J Endocrinol. 1977; 74:47–55. [PubMed: 874417]

Lasnitzki I, Mizuno T. Prostatic induction: interaction of epithelium and mesenchyme from normal wild-type mice and androgen-insensitive mice with testicular feminization. J Endocrinol. 1980; 85:423–428. [PubMed: 7411008]

Lin TM, Rasmussen NT, Moore RW, Albrecht RM, Peterson RE. Region-specific inhibition of prostatic epithelial bud formation in the urogenital sinus of C57BL/6 mice exposed *in utero* to 2,3,7,8-tetrachlorodibenzo-*p*-dioxin. Toxicological Sciences. 2003; 76:171–181. [PubMed: 12944588]

Liu F, Chu EY, Watt B, Zhang Y, Gallant NM, Andl T, Yang SH, Lu MM, Piccolo S, Schmidt-Ullrich R, Taketo MM, Morrisey EE, Atit R, Dlugosz AA, Millar SE. Wnt/beta-catenin signaling directs multiple stages of tooth morphogenesis. Dev Biol. 2008; 313:210–224. [PubMed: 18022614]

Lo Celso C, Prowse DM, Watt FM. Transient activation of beta-catenin signalling in adult mouse epidermis is sufficient to induce new hair follicles but continuous activation is required to maintain hair follicle tumours. Development. 2004; 131:1787–1799. [PubMed: 15084463]

Lustig B, Jerchow B, Sachs M, Weiler S, Pietsch T, Karsten U, van de Wetering M, Clevers H, Schlag PM, Birchmeier W, Behrens J. Negative feedback loop of Wnt signaling through upregulation of conductin/axin2 in colorectal and liver tumors. Mol Cell Biol. 2002; 22:1184–1193. [PubMed: 11809809]

Maretto S, Cordenonsi M, Dupont S, Braghetta P, Broccoli V, Hassan AB, Volpin D, Bressan GM, Piccolo S. Mapping Wnt/beta-catenin signaling during mouse development and in colorectal tumors. Proc Natl Acad Sci U S A. 2003; 100:3299–3304. [PubMed: 12626757]

Marker PC, Donjacour AA, Dahiya R, Cunha GR. Hormonal, cellular, and molecular control of prostatic development. Dev Biol. 2003; 253:165–174. [PubMed: 12645922]

Marose TD, Merkel CE, McMahon AP, Carroll TJ. Beta-catenin is necessary to keep cells of ureteric bud/Wolffian duct epithelium in a precursor state. Dev Biol. 2008; 314:112–126. [PubMed: 18177851]

Matsui D, Sakari M, Sato T, Murayama A, Takada I, Kim M, Takeyama K, Kato S. Transcriptional regulation of the mouse steroid 5alpha-reductase type II gene by progesterone in brain. Nucleic Acids Res. 2002; 30:1387–1393. [PubMed: 11884637]

Medici D, Hay ED, Olsen BR. Snail and Slug promote epithelial-mesenchymal transition through beta-catenin-T-cell factor-4-dependent expression of transforming growth factor-beta3. Mol Biol Cell. 2008; 19:4875–4887. [PubMed: 18799618]

Mulholland DJ, Dedhar S, Coetzee GA, Nelson CC. Interaction of nuclear receptors with the Wnt/beta-catenin/Tcf signaling axis: Wnt you like to know? Endocr Rev. 2005; 26:898–915. [PubMed: 16126938]

Murtaugh LC, Law AC, Dor Y, Melton DA. Beta-catenin is essential for pancreatic acinar but not islet development. Development. 2005; 132:4663–4674. [PubMed: 16192304]

Nakaya MA, Biris K, Tsukiyama T, Jaime S, Rawls JA, Yamaguchi TP. Wnt3a links left-right determination with segmentation and anteroposterior axis elongation. Development. 2005; 132:5425–5436. [PubMed: 16291790]

Nam JS, Turcotte TJ, Smith PF, Choi S, Yoon JK. Mouse cristin/R-spondin family proteins are novel ligands for the Frizzled 8 and LRP6 receptors and activate beta-catenin-dependent gene expression. J Biol Chem. 2006; 281:13247–13257. [PubMed: 16543246]

Nam JS, Turcotte TJ, Yoon JK. Dynamic expression of R-spondin family genes in mouse development. Gene Expr Patterns. 2007; 7:306–312. [PubMed: 17035101]

Noramly S, Freeman A, Morgan BA. beta-catenin signaling can initiate feather bud development. Development. 1999; 126:3509–3521. [PubMed: 10409498]

Oyama T, Kanai Y, Ochiai A, Akimoto S, Oda T, Yanagihara K, Nagafuchi A, Tsukita S, Shibamoto S, Ito F, et al. A truncated beta-catenin disrupts the interaction between E-cadherin and alpha-catenin: a cause of loss of intercellular adhesiveness in human cancer cell lines. Cancer Res. 1994; 54:6282–6287. [PubMed: 7954478]

Podlasek CA, Barnett DH, Clemens JQ, Bak PM, Bushman W. Prostate development requires Sonic hedgehog expressed by the urogenital sinus epithelium. Dev Biol. 1999; 209:28–39. [PubMed: 10208740]

Podlasek CA, Duboule D, Bushman W. Male accessory sex organ morphogenesis is altered by loss of function of Hoxd-13. Dev Dyn. 1997; 208:454–465. [PubMed: 9097018]

Pritchard C, Mecham B, Dumpit R, Coleman I, Bhattacharjee M, Chen Q, Sikes RA, Nelson PS. Conserved gene expression programs integrate mammalian prostate development and tumorigenesis. Cancer Res. 2009; 69:1739–1747. [PubMed: 19223557]

Saito M, Mizuno T. Prostatic bud induction by brief treatment with growth factors. C R Seances Soc Biol Fil. 1997; 191:261–265. [PubMed: 9255353]

Schaeffer EM, Marchionni L, Huang Z, Simons B, Blackman A, Yu W, Parmigiani G, Berman DM. Androgen-induced programs for prostate epithelial growth and invasion arise in embryogenesis and are reactivated in cancer. Oncogene. 2008; 27:7180–7191. [PubMed: 18794802]

Shannon JM, Cunha GR. Autoradiographic localization of androgen binding in the developing mouse prostate. Prostate. 1983; 4:367–373. [PubMed: 6866851]

Sheng H, Shao J, Williams CS, Pereira MA, Taketo MM, Oshima M, Reynolds AB, Washington MK, DuBois RN, Beauchamp RD. Nuclear translocation of beta-catenin in hereditary and carcinogen-induced intestinal adenomas. Carcinogenesis. 1998; 19:543–549. [PubMed: 9600336]

Southard-Smith EM, Kos L, Pavan WJ. Sox10 mutation disrupts neural crest development in Dom Hirschsprung mouse model. Nat Genet. 1998; 18:60–64. [PubMed: 9425902]

Sugimura Y, Cunha GR, Donjacour AA. Morphogenesis of ductal networks in the mouse prostate. Biol Reprod. 1986; 34:961–971. [PubMed: 3730488]

Tanner MJ, Welliver RC, Chen M, Shtutman M, Godoy A, Smith G, Mian BM, Buttyan R. Effects of androgen receptor and androgen on gene expression in prostate stromal fibroblasts and paracrine signaling to prostate cancer cells. PLoS One. 2011; 6:e16027. [PubMed: 21267466]

Thomsen MK, Butler CM, Shen MM, Swain A. Sox9 is required for prostate development. Dev Biol. 2008; 316:302–311. [PubMed: 18325490]

Thomson AA, Cunha GR. Prostatic growth and development are regulated by FGF10. Development. 1999; 126:3693–3701. [PubMed: 10409514]

van de Wetering M, Sancho E, Verweij C, de Lau W, Oving I, Hurlstone A, van der Horn K, Batlle E, Coudreuse D, Haramis AP, Tjon-Pon-Fong M, Moerer P, van den Born M, Soete G, Pals S, Eilers M, Medema R, Clevers H. The beta-catenin/TCF-4 complex imposes a crypt progenitor phenotype on colorectal cancer cells. Cell. 2002; 111:241–250. [PubMed: 12408868]

van Tienen FH, Laeremans H, van der Kallen CJ, Smeets HJ. Wnt5b stimulates adipogenesis by activating PPARgamma, and inhibiting the beta-catenin dependent Wnt signaling pathway together with Wnt5a. Biochem Biophys Res Commun. 2009; 387:207–211. [PubMed: 19577541]

Vezina CM, Allgeier SH, Fritz WA, Moore RW, Strerath M, Bushman W, Peterson RE. Retinoic acid induces prostatic bud formation. Dev Dyn. 2008a

Vezina CM, Allgeier SH, Moore RW, Lin TM, Bemis JC, Hardin HA, Gasiewicz TA, Peterson RE. Dioxin causes ventral prostate agenesis by disrupting dorsoventral patterning in developing mouse prostate. Toxicol Sci. 2008b; 106:488–496. [PubMed: 18779384]

Vezina CM, Cook C, Allgeier SH, Shaw A, Yu M, Peterson RE, Bushman W. Noggin is required for normal lobe patterning and ductal budding in the mouse prostate. Dev Biol. 2007a; 312:217–230. [PubMed: 18028901]

Vezina CM, Hicks SM, Moore RW, Peterson RE. TCDD modulates selected developmental signaling pathways during mouse prostate morphogenesis. Organohalogen Compounds. 2007b; 69:629–632.

vom Saal FS. Sexual differentiation in litter-bearing mammals: influence of sex of adjacent fetuses in utero. J Anim Sci. 1989; 67:1824–1840. [PubMed: 2670873]

Wang BE, Wang XD, Ernst JA, Polakis P, Gao WQ. Regulation of epithelial branching morphogenesis and cancer cell growth of the prostate by Wnt signaling. PLoS ONE. 2008; 3:e2186. [PubMed: 18478098]

Warot X, Fromental-Ramain C, Fraulob V, Chambon P, Dolle P. Gene dosage-dependent effects of the Hoxa-13 and Hoxd-13 mutations on morphogenesis of the terminal parts of the digestive and urogenital tracts. Development. 1997; 124:4781–4791. [PubMed: 9428414]

Widelitz RB, Jiang TX, Lu J, Chuong CM. beta-catenin in epithelial morphogenesis: conversion of part of avian foot scales into feather buds with a mutated beta-catenin. Dev Biol. 2000; 219:98–114. [PubMed: 10677258]

Willert J, Epping M, Pollack JR, Brown PO, Nusse R. A transcriptional response to Wnt protein in human embryonic carcinoma cells. BMC Dev Biol. 2002; 2:8. [PubMed: 12095419]

Wu X, Daniels G, Shapiro E, Xu K, Huang H, Li Y, Logan S, Greco MA, Peng Y, Monaco ME, Melamed J, Lepor H, Grishina I, Lee P. LEF1 Identifies Androgen-Independent Epithelium in the Developing Prostate. Mol Endocrinol. 2011; 25:1018–1026. [PubMed: 21527502]

Yu X, Wang Y, Jiang M, Bierie B, Roy-Burman P, Shen MM, Taketo MM, Wills M, Matusik RJ. Activation of beta-Catenin in mouse prostate causes HGPIN and continuous prostate growth after castration. Prostate. 2009; 69:249–262. [PubMed: 18991257]

Zhang TJ, Hoffman BG, Ruiz de Algara T, Helgason CD. SAGE reveals expression of Wnt signalling pathway members during mouse prostate development. Gene Expr Patterns. 2006; 6:310–324. [PubMed: 16378759]

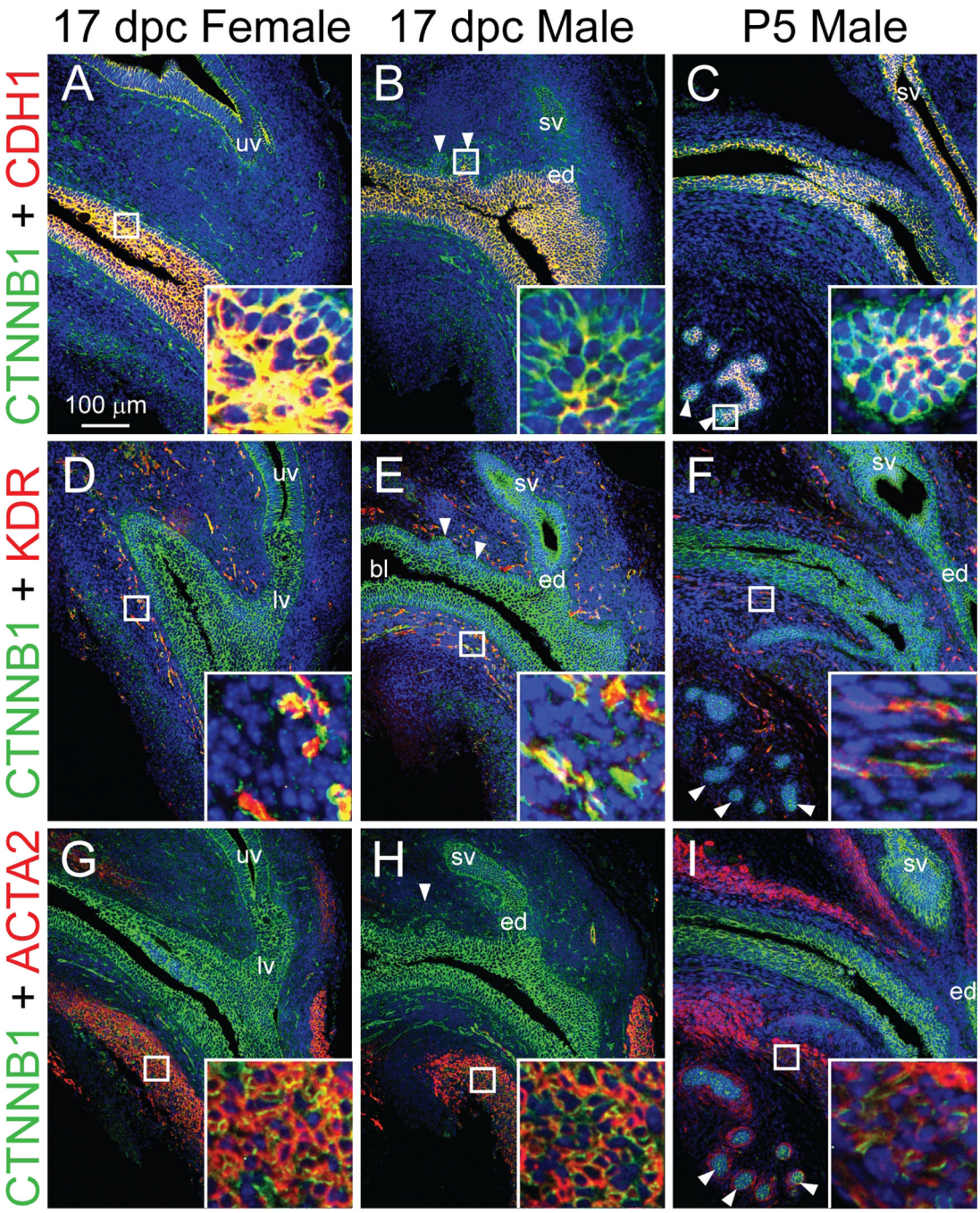

Fig. 1.

β-catenin protein expression pattern in developing mouse LUT. 17 dpc male and female mouse LUT near-mid sagittal sections (5 μm) were stained by immunofluorescence to visualize β-catenin (CTNNB1, green) and (**A–C**) the epithelial cell marker cadherin 1 (CDH1, red), (**D–F**) the vascular endothelium marker kinase insert domain protein receptor (KDR, red), and (**G–I**) the smooth muscle marker actin alpha 2 (ACTA2, red). Cell nuclei were stained with DAPI (blue). Staining patterns in each panel are representative of three males and three females. Abbreviations used are BL: bladder, ED: ejaculatory duct, LV:

lower vagina, SV, seminal vesicle, UV: upper vagina. White arrowheads indicate prostatic buds. Insets contain magnified images.

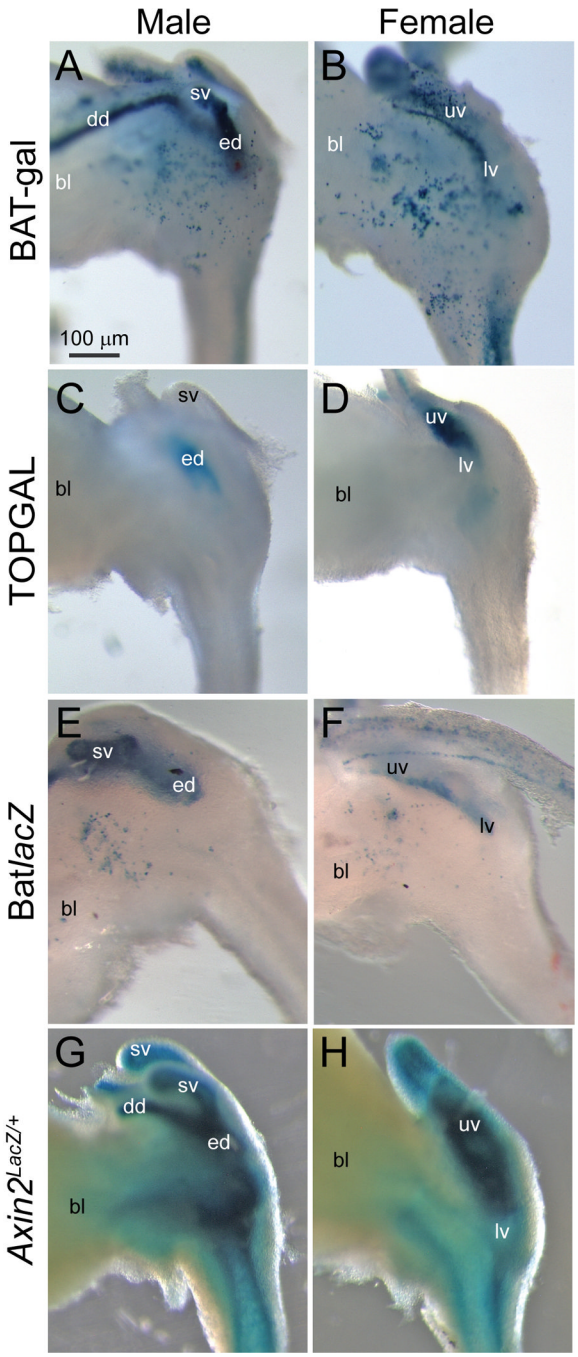

Fig. 2.

WNT/β-catenin-responsive gene expression patterns in developing transgenic mouse LUT. β-galactosidase activity (blue) in whole-mount 17 dpc male and female LUT was assessed in four different WNT/β-catenin-responsive reporter mouse strains: (**A–B**) BAT-gal (Maretto et al., 2003), (**C–D**) TOPGAL (DasGupta and Fuchs, 1999), (**E–F**) Bat*lacZ* (Nakaya et al., 2005) and (**G–H**) *Axin2*$^{LacZ/+}$(Lustig et al., 2002). Results in each panel are representative of at least two mice. Abbreviations used are BL: bladder, DD: ductus deferens, ED: ejaculatory duct, LV: lower vagina, SV, seminal vesicle, UV: upper vagina. All images are of the same magnification.

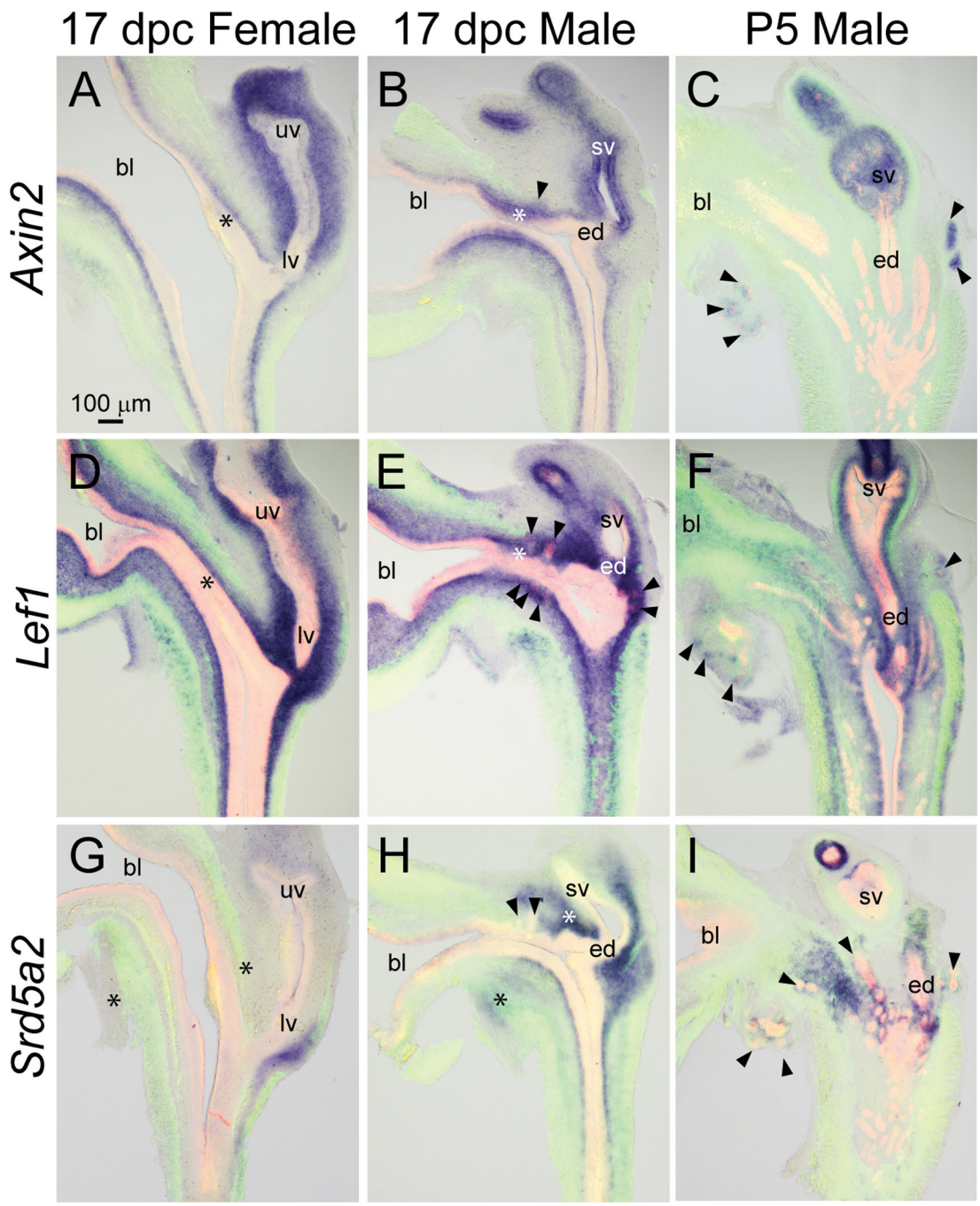

Fig. 3.

WNT/β-catenin- and androgen-responsive mRNA expression patterns in developing and neonatal mouse LUT. Near mid-sagittal sections (50 μm) of 17 dpc male and female LUT and postnatal day 5 prostate were stained by ISH to visualize mRNA expression (purple) patterns of WNT/β-catenin-responsive (**A–C**) *Axin2* and (**D–F**) *Lef1* mRNA, and (**G–I**) AR-dependent steroid 5 alpha reductase type 2 (*Srd5a2*). Sections were then stained by immunofluorescence with an anti-smooth muscle actin alpha 2 (ACTA2) antibody that recognizes muscularis mucosa and muscularis propria (green) and an anti-cadherin 1 (CDH1) antibody that recognizes all urothelium (red). Results in each panel are representative of three males and three females. Arrowheads indicate prostatic buds.

Asterisks indicate regions of sexually dimorphic mRNA expression. Abbreviations used are BL: bladder, ED: ejaculatory duct, LV: lower vagina, SV: seminal vesicle, UV: upper vagina. All images are of the same magnification.

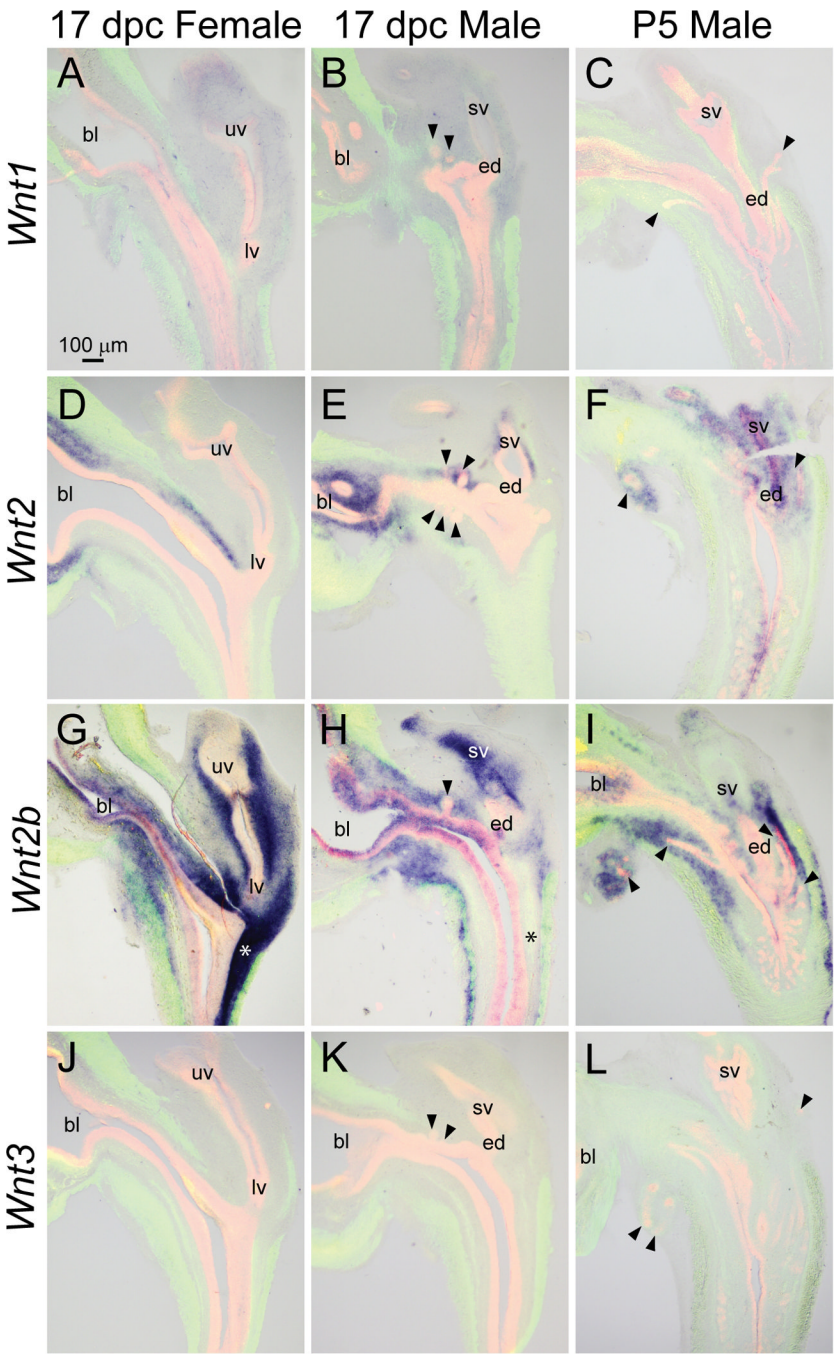

Fig. 4.

Wnt1, 2, 2b, and *3* mRNA expression patterns in developing and neonatal mouse LUT. Near mid-sagittal sections (50 μm) of 17 dpc male and female LUT and postnatal day 5 prostate were stained by ISH to visualize mRNA expression (purple) patterns of (**A–C**) wingless-related MMTV integration site 1 (*Wnt1*), (**D–F**) *Wnt2*, (**G–I**) *Wnt2b*, and (**J–L**) *Wnt3*. Sections were then stained by immunofluorescence with an anti-smooth muscle actin alpha 2 (ACTA2) antibody that recognizes muscularis mucosa and muscularis propria (green) and an anti-cadherin 1 (CDH1) antibody that recognizes all urothelium (red). Results in each panel are representative of three males and three females. Arrowheads indicate prostatic buds. Asterisks indicate regions of sexually dimorphic mRNA expression. Abbreviations

used are BL: bladder, ED: ejaculatory duct, LV: lower vagina, SV: seminal vesicle, UV: upper vagina. All images are of the same magnification.

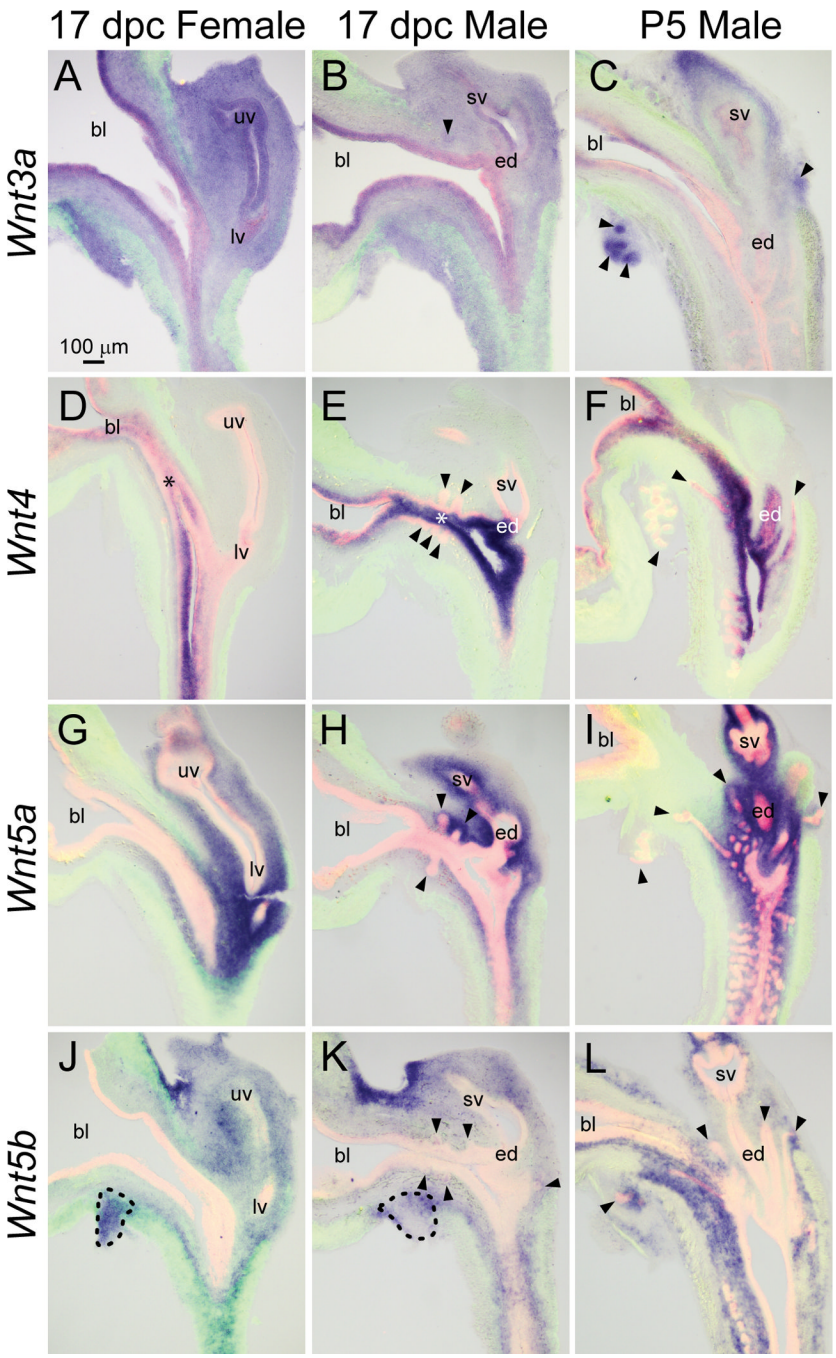

Fig. 5.

Wnt3a, 4, 5a, and *5b* mRNA expression patterns in developing and neonatal mouse LUT. Near mid-sagittal sections (50 μm) of 17 dpc male and female LUT and postnatal day 5 prostate were stained by ISH to visualize mRNA expression (purple) patterns of (**A–C**) wingless-related MMTV integration site 3a (*Wnt3a*), (**D–F**) *Wnt4*, (**G–I**) *Wnt5a*, and (**J–L**) *Wnt5b*. Sections were then stained by immunofluorescence with an anti-smooth muscle actin alpha 2 (ACTA2) antibody that recognizes muscularis mucosa and muscularis propria (green) and an anti-cadherin 1 (CDH1) antibody that recognizes all urothelium (red). Results in each panel are representative of three males and three females. Arrowheads indicate prostatic buds. Asterisks indicate regions of sexually dimorphic mRNA expression.

Mesenchymal pads are indicated by dashed lines. Abbreviations used are BL: bladder, ED: ejaculatory duct, LV: lower vagina, SV: seminal vesicle, UV: upper vagina. All images are of the same magnification.

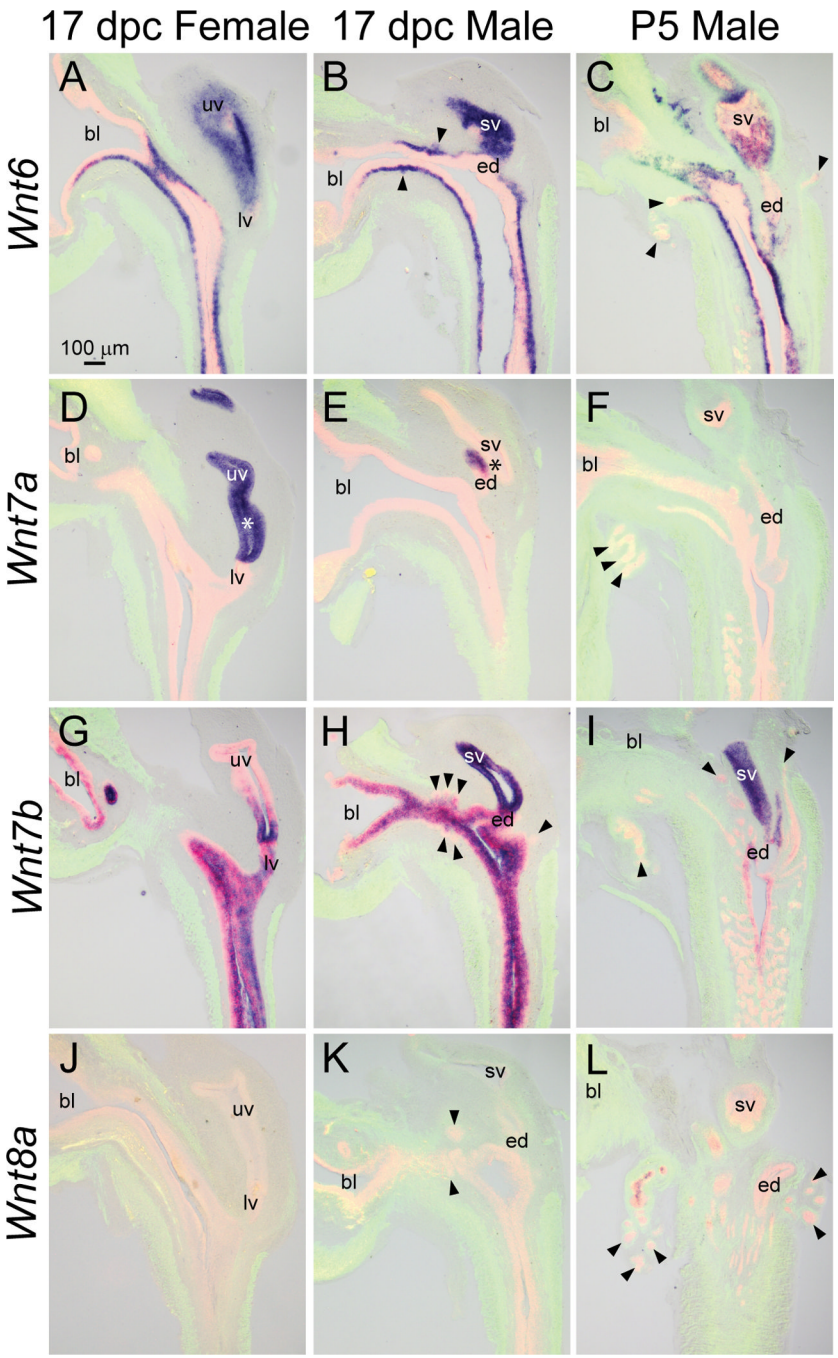

Fig. 6.

Wnt6, 7a, 7b, and *8a* mRNA expression patterns in developing and neonatal mouse LUT. Near mid-sagittal sections (50 μm) of 17 dpc male and female LUT and postnatal day 5 prostate were stained by ISH to visualize mRNA expression (purple) patterns of (**A–C**) wingless-related MMTV integration site 6 (*Wnt6*), (**D–F**) *Wnt7a*, (**G–I**) *Wnt7b*, and (**J–L**) *Wnt8a*. Sections were then stained by immunofluorescence with an anti-smooth muscle actin alpha 2 (ACTA2) antibody that recognizes muscularis mucosa and muscularis propria (green) and an anti-cadherin 1 (CDH1) antibody that recognizes all urothelium (red). Results in each panel are representative of three males and three females. Arrowheads indicate

prostatic buds. Asterisks indicate regions of sexually dimorphic mRNA expression. Abbreviations used are BL: bladder, ED: ejaculatory duct, LV: lower vagina, SV: seminal vesicle, UV: upper vagina. All images are of the same magnification.

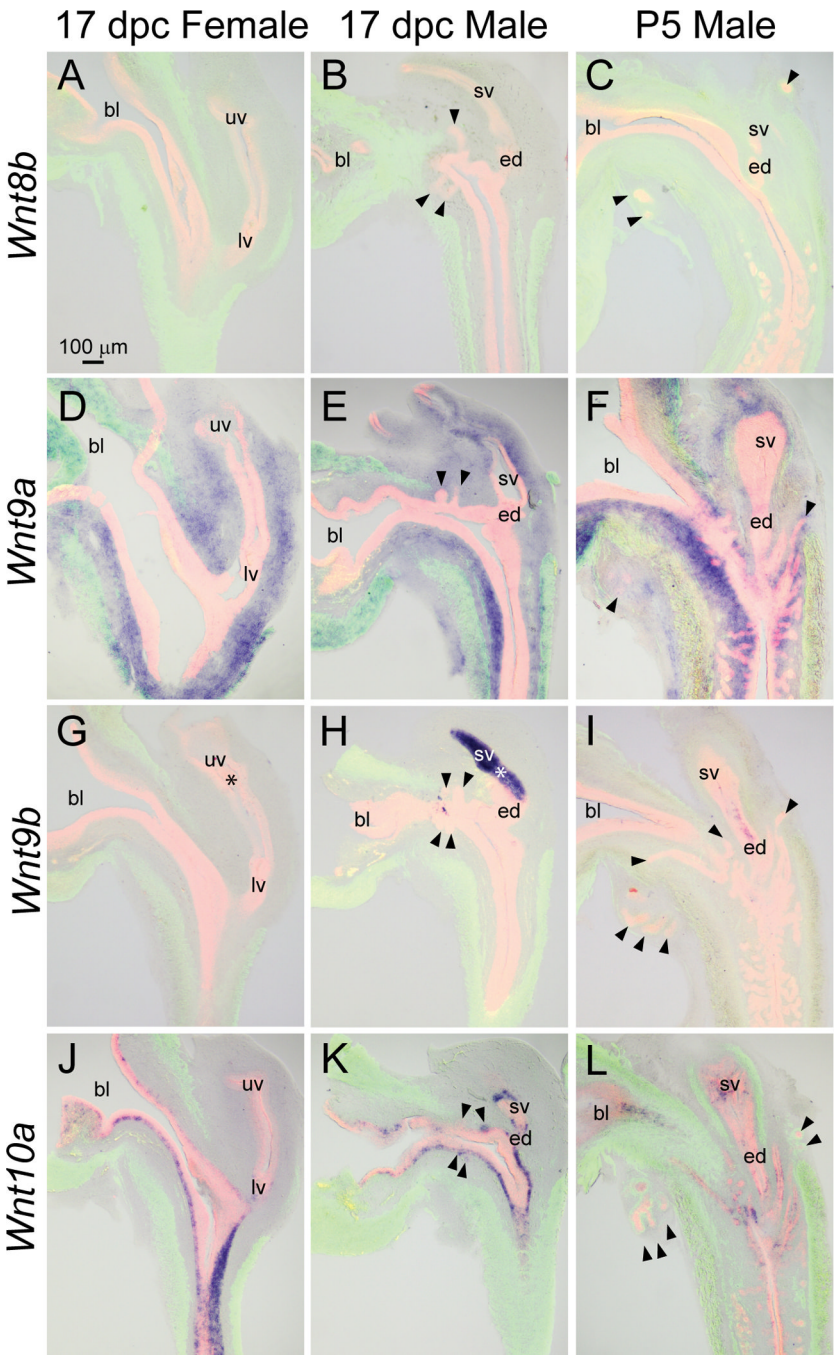

Fig. 7.

Wnt8b, 9a, *9b*, and *10a* mRNA expression patterns in developing and neonatal mouse LUT. Near mid-sagittal sections (50 μm) of 17 dpc male and female LUT and postnatal day 5 prostate were stained by ISH to visualize mRNA expression (purple) patterns of (**A–C**) wingless-related MMTV integration site 8b (*Wnt8b*), (**D–F**) *Wnt9a*, (**G–I**) *Wnt9b*, and (**J–L**) *Wnt10a*. Sections were then stained by immunofluorescence with an anti-smooth muscle actin alpha 2 (ACTA2) antibody that recognizes muscularis mucosa and muscularis propria (green) and an anti-cadherin 1 (CDH1) antibody that recognizes all urothelium (red). Results in each panel are representative of three males and three females. Arrowheads indicate

prostatic buds. Asterisks indicate regions of sexually dimorphic mRNA expression. Abbreviations used are BL: bladder, ED: ejaculatory duct, LV: lower vagina, SV: seminal vesicle, UV: upper vagina. All images are of the same magnification.

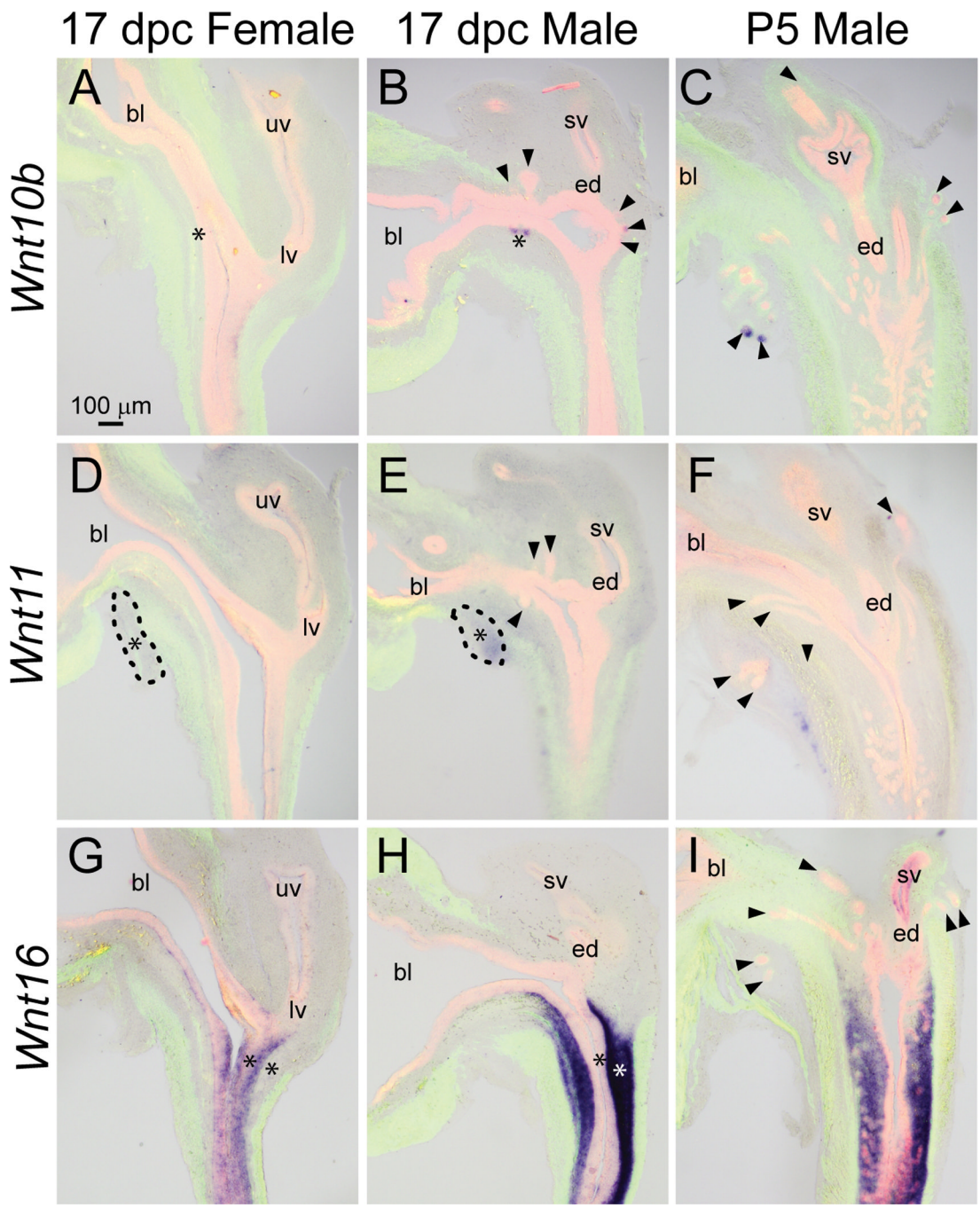

Fig. 8.

Wnt10b, 11, and *16* mRNA expression patterns in developing and neonatal mouse LUT. Near mid-sagittal sections (50 μm) of 17 dpc male and female LUT and postnatal day 5 prostate were stained by ISH to visualize mRNA expression (purple) patterns of (**A–C**) wingless-related MMTV integration site 10b (*Wnt10b*), (**D–F**) *Wnt11*, and (**G–I**) *Wnt16*. Sections were then stained by immunofluorescence with an anti-smooth muscle actin alpha 2 (ACTA2) antibody that recognizes muscularis mucosa and muscularis propria (green) and an anti-cadherin 1 (CDH1) antibody that recognizes all urothelium (red). Results in each panel are representative of three males and three females. Arrowheads indicate prostatic

buds. Asterisks indicate regions of sexually dimorphic mRNA expression. Mesenchymal pads are indicated by dashed lines. Abbreviations used are BL: bladder, ED: ejaculatory duct, LV: lower vagina, SV: seminal vesicle, UV: upper vagina. All images are of the same magnification.

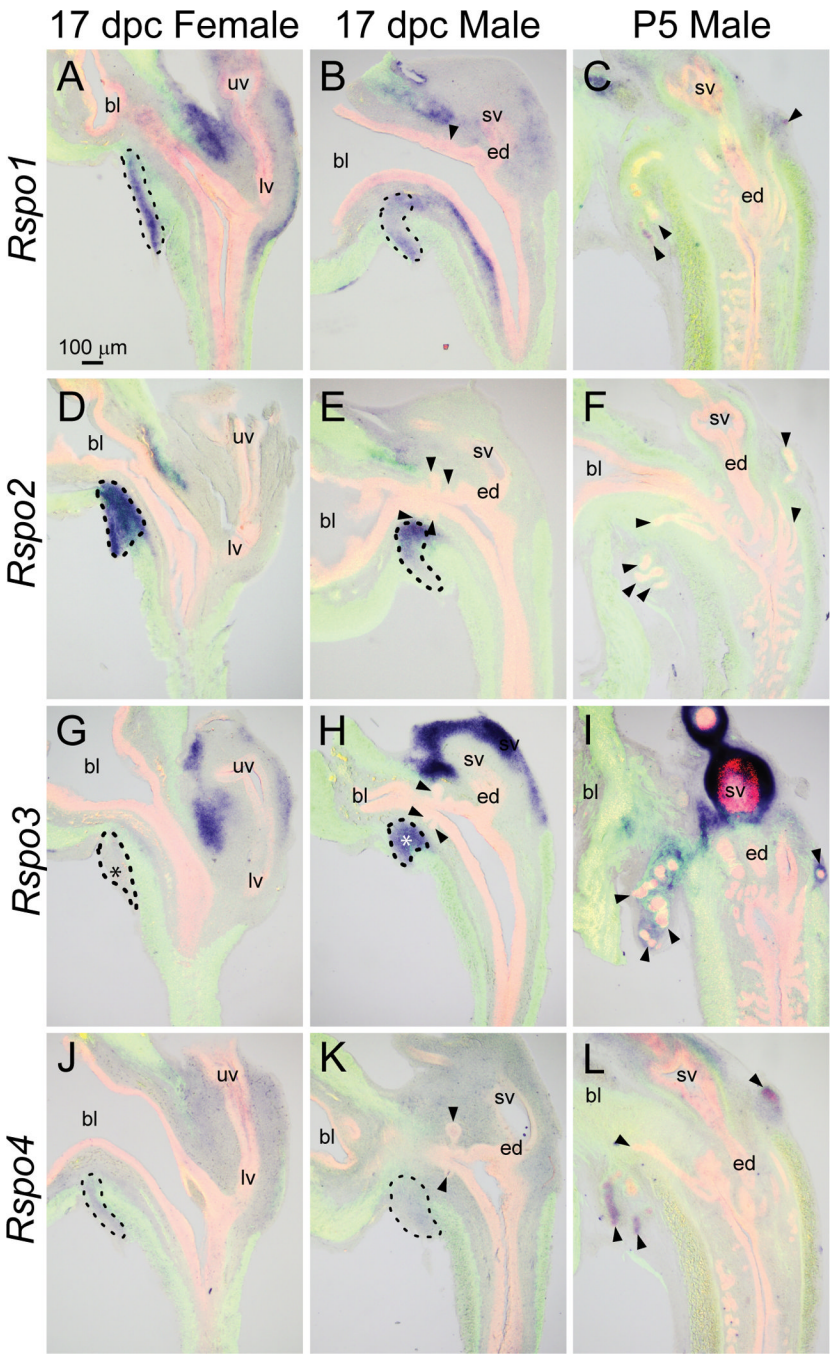

Fig. 9.

Rspo1, 2, 3, and *4* mRNA expression patterns in developing and neonatal mouse LUT. Near mid-sagittal sections (50 μm) of 17 dpc male and female LUT and postnatal day 5 prostate were stained by ISH to visualize mRNA expression (purple) patterns of (**A–C**) r-spondin homolog 1 (*Rspo1*), (**D–F**) *Rspo2*, (**G–I**) *Rspo3*, and (**J–L**) *Rspo4*. Sections were then stained by immunofluorescence with an anti-smooth muscle actin alpha 2 (ACTA2) antibody that recognizes muscularis mucosa and muscularis propria (green) and an anti-cadherin 1 (CDH1) antibody that recognizes all urothelium (red). Results in each panel are representative of three males and three females. Arrowheads indicate prostatic buds. Asterisks indicate regions of sexually dimorphic mRNA expression. Mesenchymal pads are

indicated by dashed lines. Abbreviations used are BL: bladder, ED: ejaculatory duct, LV: lower vagina, SV: seminal vesicle, UV: upper vagina. All images are of the same magnification.